Interregional synaptic competition in neurons with multiple STDP-inducing signals

Lital Bar Ilan, Albert Gidon and Idan Segev

J Neurophysiol 105:989-998, 2011. First published 1 December 2010; doi:10.1152/jn.00612.2010

You might find this additional info useful...

This article cites 65 articles, 37 of which can be accessed free at:
http://jn.physiology.org/content/105/3/989.full.html#ref-list-1

Updated information and services including high resolution figures, can be found at:
http://jn.physiology.org/content/105/3/989.full.html

Additional material and information about ***Journal of Neurophysiology*** can be found at:
http://www.the-aps.org/publications/jn

This infomation is current as of March 22, 2011.

Journal of Neurophysiology publishes original articles on the function of the nervous system. It is published 12 times a year (monthly) by the American Physiological Society, 9650 Rockville Pike, Bethesda MD 20814-3991. Copyright © 2011 by the American Physiological Society. ISSN: 0022-3077, ESSN: 1522-1598. Visit our website at http://www.the-aps.org/.

Downloaded from jn.physiology.org on March 22, 2011

J Neurophysiol 105: 989–998, 2011.
First published December 1, 2010; doi:10.1152/jn.00612.2010.

Interregional synaptic competition in neurons with multiple STDP-inducing signals

Lital Bar Ilan,[1] Albert Gidon,[1] and Idan Segev[1,2,3]

[1]*Institute of Life Sciences, Department of Neurobiology,* [2]*Center for Neural Computation, and* [3]*the Edmond and Lily Safra Center for Brain Sciences, Edmond J. Safra Campus, the Hebrew University, Givat Ram, Jerusalem, Israel*

Submitted 12 July 2010; accepted in final form 29 November 2010

Bar Ilan L, Gidon A, Segev I. Interregional synaptic competition in neurons with multiple STDP-inducing signals. *J Neurophysiol* 105: 989–998, 2011. First published December 1, 2010; doi:10.1152/jn.00612.2010.—Neocortical layer 5 (L5) pyramidal cells have at least two spike initiation zones: Na^+ spikes are generated near the soma, and Ca^{2+} spikes at the apical dendritic tuft. These spikes interact with each other and serve as signals for synaptic plasticity. The present computational study explores the implications of having two spike-timing-dependent plasticity (STDP) signals in a neuron, each with its respective regional population of synaptic "pupils." In a detailed model of an L5 pyramidal neuron, competition emerges between synapses belonging to different regions, on top of the competition among synapses within each region, which characterizes the STDP mechanism. Interregional competition results in strengthening of one group of synapses, which ultimately dominates cell firing, at the expense of weakening synapses in other regions. This novel type of competition is inherent to dendrites with multiple regional signals for Hebbian plasticity. Surprisingly, such interregional competition exists even in a simplified model of two identical coupled compartments. We find that in a model of an L5 pyramidal cell, the different synaptic subpopulations "live in peace" when the induction of Ca^{2+} spikes requires the back-propagating action potential (BPAP). Thus we suggest a new key role for the BPAP, to maintain the balance between synaptic efficacies throughout the dendritic tree, thereby sustaining the functional integrity of the entire neuron.

synaptic plasticity; calcium spike; dendrite; compartmental model; pyramidal cell

AT LEAST TWO SEPARATE SPIKE initiation zones exist in neocortical layer 5 (L5) pyramidal neurons: low-threshold Na^+ spikes are generated near the soma (Stuart and Sakmann 1994; Stuart et al. 1997b), whereas high-threshold Ca^{2+} spikes are initiated near the main bifurcation of the apical dendritic tuft (Schiller et al. 1995; Schiller et al. 1997; Helmchen et al. 1999; Larkum and Zhu 2002; see Fig. 1). These two regions interact with each other: the coincidence of synaptic inputs impinging on the apical tuft with a back-propagating action potential (BPAP; Stuart and Sakmann 1994; Spruston et al. 1995; Larkum et al. 1996) triggers a dendritic Ca^{2+} spike that, in turn, generates a burst of somatic spikes (BAC firing; Kim and Connors 1993; Buzsáki et al. 1996; Larkum et al. 1999a; Larkum et al. 1999b; Schwindt and Crill 1999; Larkum et al. 2001).

The Na^+ spike has been shown to play a key role as a postsynaptic signal for spike-timing-dependent synaptic plasticity (STDP; Bell et al. 1997; Markram et al. 1997; Dan and Poo 2006). However, recently Golding and colleagues (Golding et al. 2002; Lisman and Spruston 2005) demonstrated that synapses at the distal apical tuft undergo long-term plasticity (LTP) in the absence of somatic Na^+ spikes and that distal Ca^{2+} spikes are crucial for this LTP induction. Holthoff et al. (2004) showed that spatially restricted synaptic long-term depression (LTD) is induced by local dendritic spikes, and Remy and Spruston (2007) found that single-burst LTP depends on dendritic spikes but not on the BPAPs. Preliminary results also indicate that coincidence of synaptically induced local dendritic spikes and BPAPs produces LTP (Holthoff et al. 2006). Dendritic calcium electrogenesis was found to be necessary for LTP in the apical tree of L5 neurons (Letzkus et al. 2006), and cooperative distal synaptic inputs were shown to switch plasticity from LTD to LTP, potentially via generation of dendritic spikes (Sjöström and Häusser 2006). Ca^{2+} spikes were also shown to play an important role in determining the efficacy of the STDP induction process (Kampa et al. 2006).

If both somatic Na^+ spikes and dendritic Ca^{2+} spikes serve as signals for the induction of synaptic plasticity, an important general problem emerges: how would the spatially distributed synapses in a single neuron "manage" with two (or perhaps multiple) plasticity-inducing signals that interact with each other? This study shows that when different dendritic regions have a local Hebbian "teacher" for synaptic plasticity, STDP would not only induce competition among synapses within each (somatic or dendritic) region (Gerstner et al. 1996; Zhang et al. 1998), but also between different cell regions. Consequently, a synaptic subpopulation in one region may strengthen at the expense of synapses in the other region, undermining the functional integrity of the geometrically complex dendritic tree (Goldberg et al. 2002). In other words, interregional competition effectively creates two distinct synaptic populations, which differ in the probability of synapses within each population to become potentiated or depressed. In contrast, with one group of synapses and one STDP-inducing rule, this probability is equal among all synapses.

This study shows that interdendritic competition is inherent to multiple STDP-inducing signals operating in different regions of the same neuron. The emergence of such competition depends on the electrical coupling between the different dendritic regions. Above a critical degree of coupling, the different synaptic populations begin to compete, which results in the potentiation of one population of synapses at the expense of the other.

As the effective coupling between soma and dendrites in L5 pyramidal cells can be controlled by tuning the density of Na^+ channels in the apical trunk, we suggest a novel role for the

Address for reprint requests and other correspondence: I. Segev, Dept. of Neurobiology, The Hebrew Univ., Edmond J. Safra Campus, Givat Ram, Jerusalem 91904, Israel (e-mail: idan@lobster.ls.huji.ac.il).

0022-3077/11 Copyright © 2011 the American Physiological Society

Downloaded from jn.physiology.org on March 22, 2011

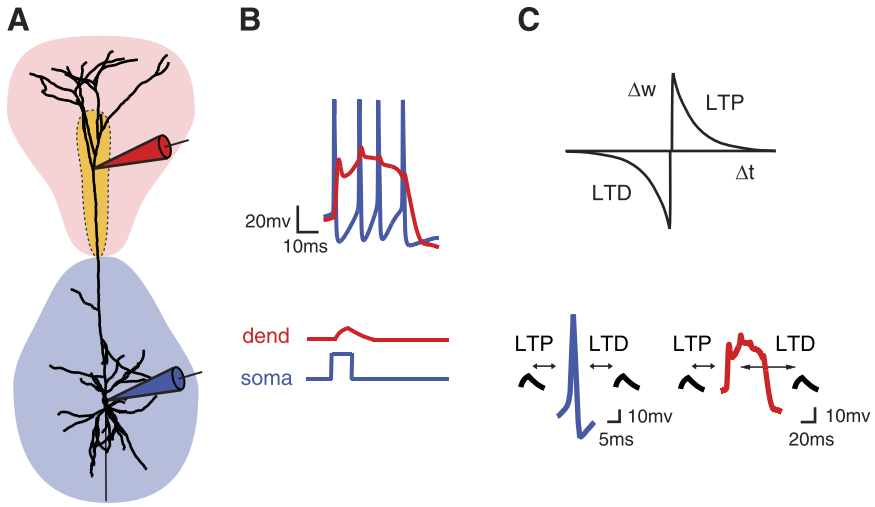

Fig. 1. Detailed model of a neocortical layer 5 (L5) pyramidal cell with 2 spike-timing-dependent plasticity (STDP)-inducing signals. *A*: a reconstructed L5-modeled cell (Schaefer et al. 2003) divided into 2 regions: a proximal region (blue) with a Na^+ spike serving as the STDP-inducing signal for synapses and a distal region (pink) with a Ca^{2+} spike serving as the signal for STDP. Orange marks the spatial distribution of low-voltage-activated (LVA) Ca^{2+} channels ("hot dendritic region"; see MATERIALS AND METHODS). *B*: voltage traces in the soma (blue) and in the main apical bifurcation (red), depicting a burst of somatic spikes (BAC firing), whereby a Ca^{2+} spike in the dendrite (dend) generates a burst of 3 additional somatic Na^+ spikes, following the coincident stimulation of the soma and the apical dendrite (*bottom* traces). *C*: the synaptic learning rule. *Top*: the STDP modification function (see MATERIALS AND METHODS). *Bottom*: timing of plasticity is relative to the onset of the somatic Na^+ spike (blue) for proximal synapses and relative to the onset of the Ca^{2+} spike (red) for the distal synapses. A total of 288 excitatory synapses were uniformly distributed over the dendrites (194 in the proximal region and 94 in the distal region). See parameters for ion channels, synapses, and the STDP rule in MATERIALS AND METHODS. LTP, long-term potentiation; LTD, long-term depression; Δw, change in synaptic weight; Δt, change in time.

BPAP, to maintain the balance between synaptic efficacies throughout the dendritic tree and sustain the functional integrity of the entire neuron.

MATERIALS AND METHODS

All simulations were designed and run using NEURON 5.8 (Hines and Carnevale 1997). Two neuron models were used in this work: that of a reconstructed L5 neocortical pyramidal cell (Fig. 1; kindly provided by A. Schaefer) and a simplified model consisting of two electrically coupled isopotential compartments, one representing the soma and the other representing the distal apical dendritic region.

Detailed compartmental model. The reconstructed L5 pyramidal cell model used in this work generates both Na^+ spikes at the axon/soma region and Ca^{2+} spikes in the vicinity of the main apical bifurcation of the apical tuft as well as back-propagation of Na^+ spikes (BPAP) and BAC firing, as found experimentally (Schaefer et al. 2003). The passive and active properties were kept as in Schaefer et al. (2003) except for several adjustments made to the calcium density in the apical tuft. The Ca^{2+} hot region included all the branches at a distance of 450–900 μm from the soma (orange region in Fig. 1*A*), the low-threshold T-type Ca^{2+} channel density was set to $\bar{g}_{LVA\text{-}Ca} = 10$ pS/μm^2, and the density of the high-threshold Ca^{2+} channel ($\bar{g}_{HVA\text{-}Ca}$) to 12 pS/μm^2. In the tuft dendrites more distal than 900 μm from the soma, the low-threshold Ca^{2+} channel conductance was either 5 pS/μm^2 (Fig. 2, *C* and *D*, and Fig. 3, "distal dominance") or absent (Fig. 2, *A* and *B*, Fig. 3, "proximal dominance," and Fig. 4). Maximal compartment size in the reconstructed L5 neuron was $\leq$20 μm, and the integration time step in all simulations was 0.025 ms.

Simplified model. This model consists of two morphologically identical spherical (diameter = 10 μm) electrically coupled compartments. The compartments were electrically connected via an adjustable resistor (R_c; Fig. 5*A*), thus controlling the coupling coefficient (CC; defined under passive conditions as V_2/V_1, where V_2 is the attenuated voltage response in the second compartment following steady-state voltage change, V_1, in the first compartment). Specific membrane capacitance was set to $C_m = 1$ μF/cm^2, and passive leak conductance (R_m) to 10,000 Ω·cm^2. Spikes at the somatic compartment were modeled using the Hodgkin and Huxley (H&H) formalism (Hodgkin and Huxley 1952) with a channel density of $\bar{g}_{Na} = 1200$ pS/μm^2 and $\bar{g}_K = 360$ pS/μm^2. The dendritic compartment contained H&H channels with lower channel densities ($\bar{g}_{Na} = 50$ pS/μm^2 and $\bar{g}_K = 5$ pS/μm^2) to account for back-propagation but to avoid the generation of a full-blown Na^+ spike in the dendrite. Three additional ion channels were used for the regenerative Ca^{2+} potentials in the dendritic compartment (Schaefer et al. 2003): low-threshold T-type Ca^{2+} channels with $\bar{g}_{LVA\text{-}Ca} = 0$–50 pS/$\mu$m^2 (Fig. 5*C*), A-type potassium current ($\bar{g}_{KA} = 700$ pS/μm^2), and high-threshold Ca^{2+} channels ($\bar{g}_{HVA\text{-}Ca} = 10$ pS/μm^2; Fig. 5).

Synapses and synaptic plasticity. Fast excitatory synaptic conductance was modeled as a single exponential (the built-in NEURON point process ExpSyn) with a time constant of 5 ms for decay of synaptic conductance and synaptic reversal potential of 0 mV (resting potential was set to −65 mV). In the detailed compartmental model (Figs. 1–4), 288 excitatory synapses were uniformly distributed per unit area over the cell surface, each with a maximal conductance of $\bar{g}_{syn} = 2$ nS, and activation times were drawn from a random Poisson process with a mean rate of 10 Hz. In the simplified two-compartment model (Figs. 5 and 6), 300 excitatory synapses impinged on each compartment, with a maximal conductance of $\bar{g}_{syn} = 0.1$ nS and an average input rate of 3 Hz. For each synapse, a weight parameter (w) was defined as

$$w = \bar{g}_{syn}/\bar{g}_{max} \quad (1)$$

where $\bar{g}_{syn}$ is the peak synaptic conductance, modifiable by STDP, and $\bar{g}_{max}$ is the upper limit for potentiation of the synapse ($0 \leq \bar{g}_{syn} \leq \bar{g}_{max}$), which was identical for all synapses. The synaptic w was initially set to 0.5 for all synapses and was modified according to the temporal difference between the synaptic input and the postsynaptic spike (either the Na^+ or the Ca^{2+} spike) according to STDP *Eqs. 2* and *3* (Song et al. 2000),

$$\Delta w_- = A_- \exp\left(-\frac{t_{post} - t_{pre}}{\tau}\right) \text{ if } t_{post} \leq t_{pre} \quad (2)$$

Downloaded from jn.physiology.org on March 22, 2011

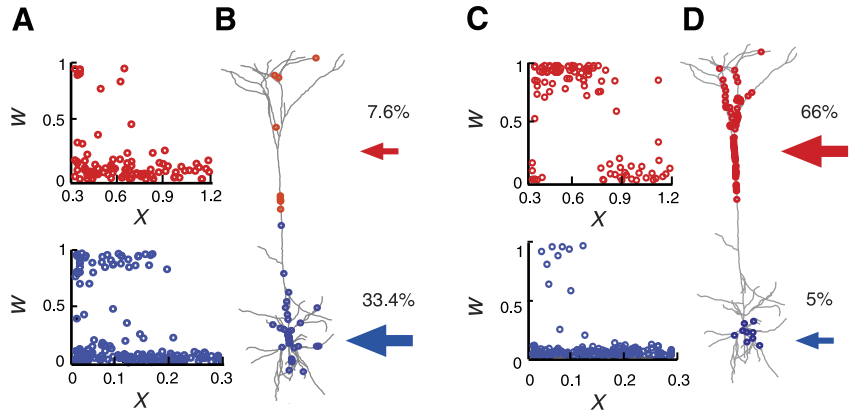

Fig. 2. Competition between proximal and distal synapses with 2 STDP-inducing signals in a detailed L5 model neuron. *A*: synaptic weights (w) as a function of electrotonic distance from the soma (X). Proximal synapses (*bottom*, blue) dominate over distal synapses (*top*, red) when the back-propagating action potential (BPAP) is sufficiently strong to independently elicit a Ca^{2+} spike (sodium conductance at the trunk was $\bar{g}_{Na} = 54$ pS/μm^2). *B*: schematic depiction of synaptic weights with respect to their location on the cell corresponding to the results in *A*. Red circles: strong distal synapses ($w > 0.5$). Blue circles: strong proximal synapses. The red arrows point to the distal region of the cell, and the blue arrows point to the proximal cell region. The percentage of strong synapses in each dendritic region is indicated above the arrows. *C*: distal synapses dominate when the excitability of the distal region is enhanced, in this case by adding T-type Ca^{2+} channels around the hot region at the distal dendritic tuft ($\bar{g}_{LVA\text{-}Ca} = 5$ pS/μm^2) and by weakening the BPAP (trunk $\bar{g}_{Na} = 27$ pS/μm^2). In this case, 66% of the distal synapses (red) were strong, whereas only 5% of the proximal synapses (blue) were strengthened at steady state. *D*: schematic depiction of synaptic weights corresponding to results in *C*.

$$\Delta w_+ = A_+ \exp\left(-\frac{t_{post} - t_{pre}}{\tau}\right) \quad \text{if} \quad t_{post} > t_{pre} \tag{3}$$

where $\Delta w_{+/-}$ is an increment/decrement in w, $A_{+/-}$ is the amplitude of synaptic potentiation/depression, t_{pre} is the time of synaptic input activation, and t_{post} is the time of the postsynaptic spike (either the Na^+ or Ca^{2+} spike). The time constant (τ) was 20 ms for both potentiation and depression. A_+ and A_- were set to 0.005 and 0.00525, respectively. A_- was slightly larger than A_+ to obtain competition in the case where STDP is the only source for depression (Debanne et al. 1998; Feldman 2000; van Rossum et al. 2000).

In the detailed L5 cell model (Figs. 1–4), the onset time, t_{post}, for the postsynaptic spike(s) was determined as the time when a predefined voltage threshold was crossed. For proximal synapses (synapses within the blue region in Fig. 1*A*), the somatic Na^+ spike served as the STDP-inducing signal, and t_{post} was set to be the time at which somatic voltage crossed the value of 0 mV. For distal synapses (within the pink area in Fig. 1*A*), the Ca^{2+} spike served for STDP induction, and t_{post} was the time at which voltage at the main apical bifurcation crossed −30 mV. In the simplified two-compartment model, each synapse underwent plasticity according to the spike in its respective compartment. In both compartments, t_{post} was deter-

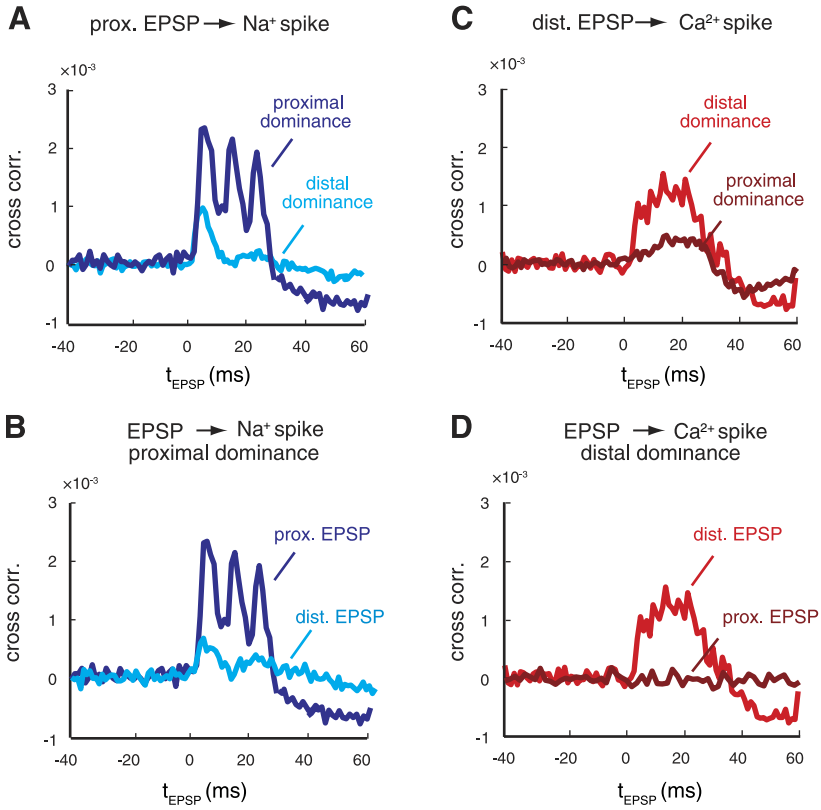

Fig. 3. Input-output correlations at initial conditions explain weight distribution at steady state. Normalized cross-correlation (cross corr.) between either proximal (prox.) or distal (dist.) excitatory postsynaptic potentials (EPSPs) occurring at t_{EPSP} and either somatic or dendritic spikes (see MATERIALS AND METHODS). Spike onset is defined as *time 0*. *A*: normalized cross-correlation between proximal synapses and somatic spikes. Under conditions leading to proximal dominance (blue), correlation was much higher than under conditions that led to distal dominance (cyan). Note that in the former case, proximal synapses were correlated with the whole burst of action potentials that followed the dendritic Ca^{2+} spike. *B*: normalized cross-correlation between dendritic synapses and the Ca^{2+} spike. Correlation was larger in the case of distal dominance (red) than for proximal dominance conditions (maroon). *C*: normalized cross-correlation between proximal synapses and somatic spikes (blue) or between distal synapses and somatic spikes (cyan) under conditions leading to proximal dominance. *D*: normalized cross-correlation between distal synapses and somatic spikes (red) or between proximal synapses and somatic spikes (maroon) in the case of distal dominance.

Downloaded from jn.physiology.org on March 22, 2011

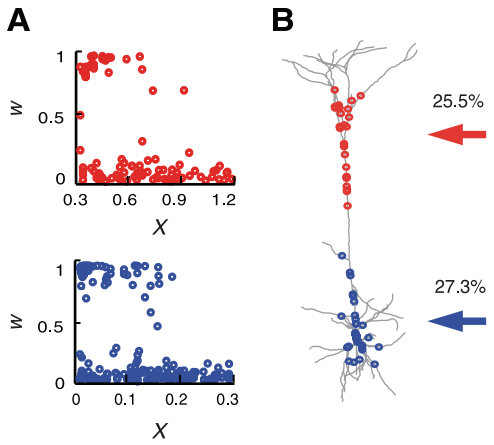

Fig. 4. Conditions for the "coexistence" of distal and proximal synaptic populations. *A*: synaptic weights (w) as a function of electronic distance from the soma (X). *B*: schematic depiction of synaptic weights with respect to their location on the cell corresponding to the results in *A*. *A* and *B*: both proximal and distal synaptic populations "coexist" such that the efficacy of a significant percentage of synapses in both populations is high. This is the case when the temporal coincidence of the BPAP and distal synaptic inputs is required for the generations of the Ca^{2+} spike (BAC firing). In this example, trunk $\bar{g}_{Na} = 27$ pS/μm^2 without T-type Ca^{2+} channels outside the hot region. Under these conditions, 25.5% of the distal synapses (red) and 27.3% of the proximal synapses (blue) were potentiated following STDP.

mined according to the onset time of the local spike, as in the detailed model explained above. In both the soma and dendrites, results were consistent regardless of the particular voltage threshold for initiating synaptic plasticity, provided that the excitatory postsynaptic potentials (EPSPs) on their own did not induce plasticity.

We used "all to all" spike interactions (Bi 2002) where the synaptic weight update was computed by the summation of Δws over all possible combinations of pairing between presynaptic and postsynaptic spikes. When steady state was reached, the synaptic weights attained a bimodal distribution (Figs. 2 and 4–6) in which most of the synapses were either maximally weak ($w \approx 0$) or maximally strong ($w \approx 1$) (Song et al. 2000).

Unless otherwise mentioned, the additive STDP rule was used. We also used another variation, the "multiplicative" STDP rule (van Rossum et al. 2000; Gutig et al. 2003). In the multiplicative case, a term that involves the dependence of STDP on the value of synaptic weights was added to *Eqs. 2* and *3* above,

$$\Delta w_+ = (1 - w)^{\mu} \times A_+ \exp\left[-(t_{post} - t_{pre})/\tau\right] \text{ if } t_{post} \geq t_{pre} \quad (4)$$

$$\Delta w_- = w^{\mu} \times A_- \exp\left[-(t_{post} - t_{pre})/\tau\right] \text{ if } t_{post} < t_{pre} \quad (5).$$

In this case, the degree of potentiation of already strong synapses is smaller than the degree of their depression and vice versa for weak synapses. The power μ determines the degree of dependence of the plasticity on the current synaptic weights; μ ranges between 0 (additive) and 1 (fully multiplicative).

The computing resources included 32-bit Intel and 64-bit AMD computers. A backward Euler integration method (NEURON default) was used. A typical simulation run time until the synaptic strengths reached steady state was between 2 h for the simplified model and 6 days for the reconstructed neuron models. Simulation time was always equal to or greater than 2×10^4 s. We determined that the model reached steady state after a reasonable amount of time had passed, in which the synaptic distribution did not change significantly.

Cross-correlation between input and output. To calculate the causal relationship between EPSPs and spikes, we used a normalized cross-correlation measure (Fig. 3). The voltage trace at either the soma or the apical main bifurcation was divided into discrete time bins of 1 ms each. If a spike appeared within this time bin, it was assigned a value of 1; otherwise, it was assigned a value of 0. A time

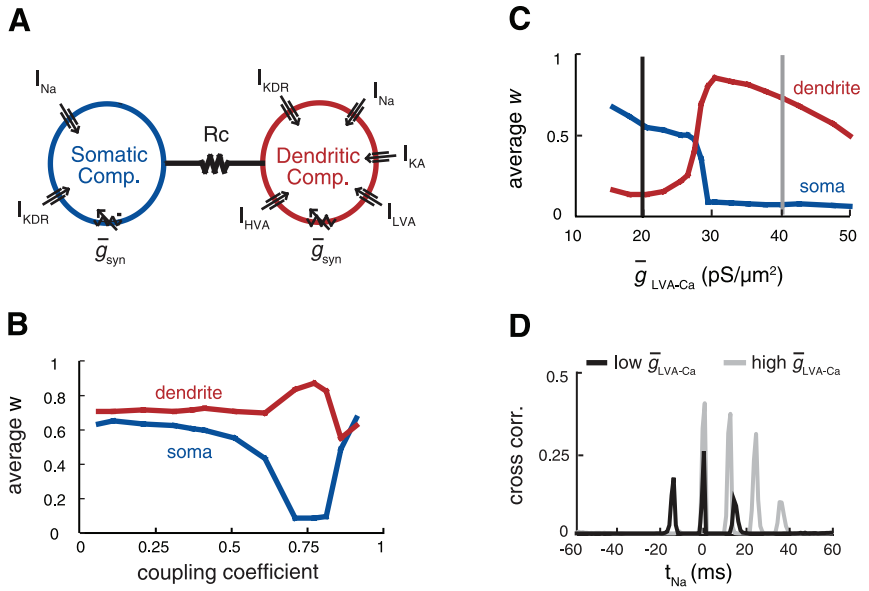

Fig. 5. Competition between 2 synaptic populations in a simplified L5 neuron model. *A*: a simplified cell model consisting of 2 morphologically identical isopotential compartments coupled by R_c resistance. The somatic compartment (blue) generated Na^+ spikes, and the dendritic compartment (red) produced Ca^{2+} spikes (see MATERIALS AND METHODS). Each compartment received 300 excitatory synapses denoted by $\bar{g}_{syn}$, activated randomly at 3 Hz. *B*: average synaptic weights at steady state as a function of the coupling coefficient (CC). For CC < 0.6, synapses at both compartments "coexisted." For midrange values of CC, competition between the 2 synaptic population ensued, leading to complete domination of the dendritic synapses in the case shown [low-threshold T-type Ca^{2+} channel density ($\bar{g}_{LVA-Ca}$) = 30 pS/μm^2]. *C*: the effect of T-type Ca^{2+} channel density on interregional competition. *D*: normalized cross-correlation between the somatic Na^+ spike occurring at t_{Na} and the dendritic Ca^{2+} spike occurring at *time 0*, with low $\bar{g}_{LVA-Ca}$ (20 pS/μm^2; black curve corresponds to the vertical black line in *C*) or high $\bar{g}_{LVA-Ca}$ (40 pS/μm^2; gray curve corresponds to the gray vertical line in *C*). Only with low LVA Ca^{2+} conductance (black line) did the Na^+ spike tend to occur before the Ca^{2+} spike. In addition, with high LVA Ca^{2+} conductance (gray line), more Na^+ spikes followed each Ca^{2+} spike compared with the low LVA Ca^{2+} conductance case. I_{KA}, A-type potassium current; I_{KDR}, delayed rectifier potassium current; I_{HVA}, high-voltage-activated calcium current.

Downloaded from jn.physiology.org on March 22, 2011

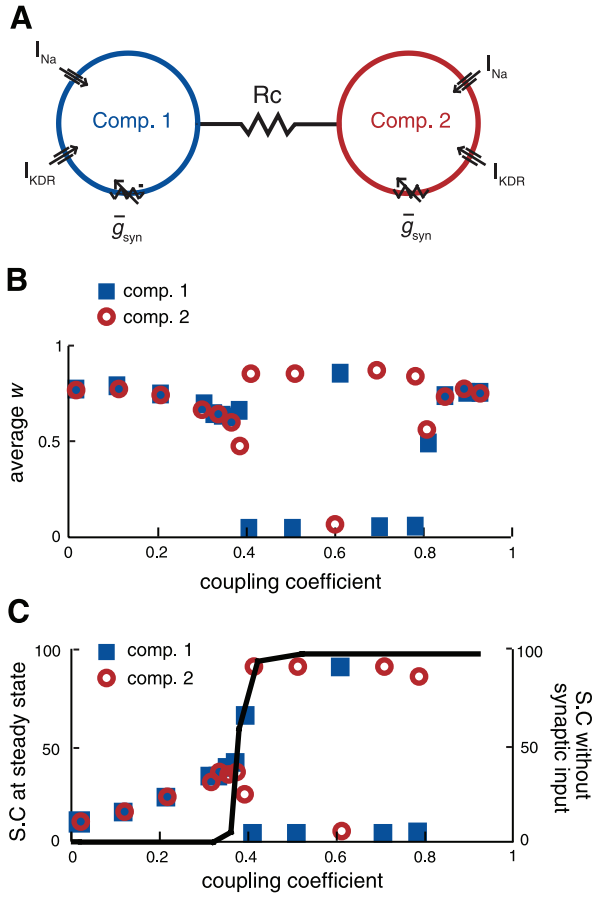

Fig. 6. Competition between 2 STDP-driven synaptic populations in a fully symmetrical case. *A*: a model consisting of 2 identical isopotential compartments (Comp.) coupled to each other by R_c resistance. Both compartments are endowed with identical Na^+-dependent spike mechanisms, and both receive 300 randomly activated excitatory synapses. *B*: average normalized synaptic weights at steady state as a function of the CC. For $0.4 < CC < 0.8$, synapses in 1 compartment became dominant at the expense of diminishing the weight of the synapses in the other compartment. The identity of the dominating group of synapses alternated randomly. *C*: spike coupling (S.C) at steady state (blue: percentage of spikes that compartment 1 induced in compartment 2; red: percentage of spikes that compartment 2 induced in compartment 1). Black line: spike coupling in the absence of synaptic activity (see MATERIALS AND METHODS).

series of 1s and 0s was also computed for each synapse: 1 signified a time bin when the synapse was activated (presynaptic spike), and 0 signified otherwise. The cross-correlation function (R_{xy}) for the ith synapse was computed as follows:

$$R^i_{xy}(k) = \sum_{n=0}^{M-k-1} \frac{(x^i_n - \mu_x)(y_{n+k} - \mu_y)}{M\sigma_x\sigma_y} \quad (6)$$

where x and y are the 0s and 1s time series for the pre- and postsynaptic spikes, respectively, μ and σ are the average and standard deviation of x and y, and k is the variable time delay. The average cross-correlation, $\bar{R}_{xy}$, was computed over all N synapses for each value of k,

$$\bar{R}_{xy}(k) = \frac{1}{N}\sum_{i=1}^{N} R^i_{xy}(k) \quad (7).$$

In Fig. 5*D*, x and y are the 0s and 1s time series of length M for the Ca^{2+} and Na^+ spikes, respectively.

Spike coupling. Spike coupling was defined as the percentage of spikes that one compartment induced in the other compartment. If a spike in one compartment followed a spike in the other within a time window of 2 ms, it was defined as being caused by the other compartment. Spike coupling was measured under two conditions. In one case, it was calculated in the presence of synaptic activity after reaching steady state following STDP (Figs. 5 and 6*C*). In the other case, spike coupling was measured in the absence of synaptic activity: spikes were randomly generated in one compartment, and the percentage of these spikes that initiated spikes in the other compartment was measured (black line in Fig. 6*C*).

RESULTS

To explore the implications of having two "supervisors" for synaptic plasticity at different regions of the same neuron, we used a detailed model of a reconstructed L5 pyramidal cell (Fig. 1*A*; kindly provided by A. Schaefer; see MATERIALS AND METHODS). Excitatory synapses underwent STDP in response to either Na^+ or Ca^{2+} spikes, based on their location. Synapses at a distance smaller than 450 μm from the soma were labeled proximal (Fig. 1*A*, blue), and the somatic Na^+ spike was used as their STDP-inducing signal. The rest of the apical synapses were labeled distal (Fig. 1*A*, pink), and the Ca^{2+} spike generated at the main apical bifurcation was used as their signal for STDP (Fig. 1*C*; see MATERIALS AND METHODS).

We found that following STDP, competition ensued between cell regions. The synaptic weight distribution at steady state following STDP in the detailed model is depicted in Fig. 2. For the two cases shown, only one group of synapses "survived" (a significant number of strong synapses with $w > 0.5$ existed at steady state), whereas the efficacy of the other group of synapses was substantially diminished ($w \approx 0$ for most synapses). In Fig. 2, *A* and *B*, the proximal synapses (blue) dominate over the distal synapses (red) following STDP. In this case of proximal dominance, the BPAP was sufficiently strong to independently elicit a dendritic Ca^{2+} spike (trunk $\bar{g}_{Na} = 54$ pS/μm^2). Distal synapses were substantially suppressed, and only 7.6% of them remained as strong (or stronger) compared with their initial weight ($w = 0.5$), whereas in the proximal region, 33.4% of the synapses were strengthened. In contrast, Fig. 2, *C* and *D*, depicts the case of distal dominance, whereby distal synapses were potentiated at the expense of proximal ones, with 66% of the distal synapses strengthened at steady state, compared with a strengthening of only 5.1% of the proximal synapses. In this case, distal synapses were sufficiently strong to independently generate Ca^{2+} spikes without the aid of BPAPs. We modeled these conditions by setting the sodium conductance at the apical trunk to a small enough value ($\bar{g}_{Na} = 27$ pS/μm^2) to prevent BPAPs from crossing the Ca^{2+} spike threshold. In addition, the Ca^{2+} channel density in the very distal tuft branches, outside of the hot region, was boosted ($\bar{g}_{LVA\text{-}Ca} > 2.5$ pS/μm^2). Note that it was shown experimentally that strong current input can generate Ca^{2+} spikes independently (Schiller et al. 1997; Stuart et al. 1997a; Helmchen et al. 1999; Larkum and Zhu 2002), suggesting that correlated distal inputs might be able to produce Ca^{2+} spikes on their own.

In both cases of proximal dominance (Fig. 2, *A* and *B*) and distal dominance (Fig. 2, *C* and *D*), synapses that were close to the spike initiation site were likely to be strengthened, whereas synapses further away from the initiation zones were typically weakened (Fig. 2, *B* and *D*). This is due to cable filtering, whereby synapses close to the initiation site are more effective

Downloaded from jn.physiology.org on March 22, 2011

at initiating spikes compared with synapses located further away from it (Gidon and Segev 2009).

In another set of experiments, we used a weight-dependent (multiplicative) STDP rule (van Rossum et al. 2000; Gutig et al. 2003). In this case, we also obtained interregional synaptic competition, provided that the multiplicative parameter was low enough so it would not "clamp" synaptic strengths and abolish competition altogether (results not shown).

What determines the winning group of synapses? To better understand the aforementioned interregional competition, we measured the average cross-correlation between synapses in each region (proximal or distal) and the corresponding spike (either Na^+ or Ca^{2+}). Normalized cross-correlation was calculated in two cases: *1*) when proximal synapses dominated following STDP (Fig. 2, *A* and *B*; $\bar{g}_{Na} = 54$ pS/μm^2 in the apical trunk and $\bar{g}_{LVA\text{-}Ca} = 0$ pS/μm^2 in the tuft surrounding the hot zone); and *2*) when distal synapses dominated (Fig. 2, *C* and *D*; trunk $\bar{g}_{Na} = 27$ pS/μm^2, tuft $\bar{g}_{LVA\text{-}Ca} = 5$ pS/μm^2). We first measured the average cross-correlation between all proximal synapses and the Na^+ spike (Fig. 3*A*). In the case of proximal dominance, correlation was much stronger (Fig. 3*A*, blue) than for the case of distal dominance (Fig. 3*A*, cyan), in agreement with a larger degree of proximal potentiation at steady state for the proximal dominance conditions (Fig. 2, *A* and *B*). For this case, the cross-correlation between the proximal synapses and the somatic Na^+ spike (Fig. 3*B*, blue) was much higher compared with correlation between distal synapses and the somatic Na^+ spike (Fig. 3*B*, cyan). In addition, the cross-correlation between the proximal synapses and the Ca^{2+} spike was higher for proximal dominance conditions compared with distal dominance (results not shown). Therefore, for proximal dominance conditions, specifically when BPAPs were potent at initiating Ca^{2+} spikes, whereas distal synapses alone could not generate a dendritic spike, proximal inputs were much more correlated with both the somatic and the dendritic spikes than in the case of distal dominance conditions. We next measured the average cross-correlation between all distal synapses and the Ca^{2+} spike (Fig. 3*C*). Distal synapses were more strongly correlated with the Ca^{2+} spike under the conditions of distal dominance (Fig. 3*C*, red) than under the conditions of proximal dominance (Fig. 3*C*, maroon). This was in agreement with the larger degree of potentiation at distal synapses for the distal dominance case at steady state (Fig. 2, *C* and *D*). The correlation of the input with the Ca^{2+} spike under distal dominance conditions was much greater for distal synapses (Fig. 3*D*, red) than proximal synapses (Fig. 3*D*, maroon). The cross-correlation between distal synapses and the Na^+ spike was also higher for conditions that give rise to distal dominance than in the case of proximal dominance (results not shown). Thus, for distal dominance conditions–specifically when BPAPs were unable to initiate the Ca^{2+} spike on their own, but the distal synapses alone could generate a dendritic spike–distal inputs were much more correlated with both the dendritic and the somatic spikes than in the case of proximal dominance.

We conclude that when the BPAP is necessary and sufficient for generating the Ca^{2+} spike, proximal synapses would be strongly potentiated, because they are positively correlated with both the somatic and the dendritic spikes and thus also with the subsequent burst of somatic spikes. Since both the initial Na^+ spike and the following burst of Na^+ spikes all fall inside the STDP time window for LTP, proximal synapses would undergo strong LTP. In this case, distal synapses are initially too weak to generate Ca^{2+} spikes independently and therefore are not correlated with the local Ca^{2+} spike. This results in LTD of distal synapses and consequently in proximal dominance.

Conversely, with sufficiently high tuft $\bar{g}_{LVA\text{-}Ca}$ for initiating Ca^{2+} spikes by distal synapses alone (when the BPAP is not necessary for initiating the dendritic Ca^{2+} spike), distal inputs are positively correlated with the dendritic spike as well as with the resultant burst of somatic spikes, which leads to LTP in distal synapses. Hence, proximal synapses are uncorrelated with many of the somatic action potentials (those generated by the Ca^{2+} spike) and consequently undergo LTD, resulting in distal dominance.

Balancing interregional competition. Model parameters were adjusted to fulfill the condition, whereby the coincidence of both the BPAP and distal synaptic inputs is required for generation of dendritic Ca^{2+} spikes, namely BAC firing (Fig. 4; Larkum et al. 1999a; Larkum et al. 1999b, 2001). Under such conditions, both synaptic populations contributed to the initiation of the Ca^{2+} spike and, via BAC firing, both populations contributed to the induction of somatic Na^+ spikes. Hence, some synapses in each region were positively correlated with the respective local spike and subsequently potentiated. This resulted in "proximal-distal equality," the coexistence of the two synaptic populations. For example, in the conditions depicted in Fig. 4, 27.3% of synapses in the proximal region and 25.5% in the distal region were potentiated. It should be noted that the reduction of competition between the regions by the coincidence requirement did not reduce the competition within each region. Consequently, the bimodal distribution of synaptic weights following STDP was still observed in each region (Song et al. 2000).

Regional competition in a two-compartment model of L5 neurons. To directly test our conclusions above and explore the effect of several electrical parameters on the interregional competition, we constructed a simplified model of L5 neurons consisting of two electrically coupled compartments (soma and dendrite) with respective Na^+ and Ca^{2+} spikes serving as STDP-inducing signals (Fig. 5*A*; see MATERIALS AND METHODS). This simplified model qualitatively replicated the results obtained in the detailed model.

The effective coupling between proximal and distal regions in the detailed L5 cell model could be modulated by changes in the density of the dendritic Na^+ channels (controlling the degree of BPAP attenuation). In the simplified model, we mimic this by changing the CC between the two compartments. Figure 5*B* demonstrates that the CC is a key parameter in determining the fate of interregional competition, specifically whether somatic and dendritic synapses coexist or whether one group of synapses dominates the other. For CC < 0.6, both synaptic populations coexisted with a larger average weight for dendritic synapses (Fig. 5*B*, red) compared with somatic synapses (Fig. 5*B*, blue). This difference in average weights stems from inherent differences in the firing rates of the two types of spikes: Na^+ spikes fire at a higher rate than Ca^{2+} spikes. With the additive STDP rule, the higher the rate of firing, the lower the percentage of potentiated synapses at steady state (Abbott and Nelson 2000; Gutig et al. 2003). Coexistence of synaptic populations at this range of CC values is attributed to the

Downloaded from jn.physiology.org on March 22, 2011

relatively small degree of interaction between the two compartments. For example, with CC = 0.2, only 11.9% of the somatic firing was due to Ca^{2+} spikes, and only 9.6% of dendritic spikes were initiated following Na^+ spikes, meaning that spike coupling was very low (see MATERIALS AND METHODS). At midrange values ($0.6 < CC < 0.8$), competition emerged, and with high enough values of $\bar{g}_{LVA\text{-}Ca}$ (> 27 pS/μm^2; see Fig. 4*C*), dendritic synapses dominated (Fig. 4*B*). For instance, with CC = 0.7 and $\bar{g}_{LVA\text{-}Ca}$ = 30 pS/μm^2, the average synaptic weight was 0.06 at the soma (Fig. 4, blue) vs. 0.93 at the dendrite (Fig. 4, red). In this case, spike coupling was substantially greater: 86% of somatic spikes were initiated by Ca^{2+} spikes, whereas only 32% of Ca^{2+} spikes were initiated by somatic action potentials. With $CC > 0.8$, the two compartments effectively merged into one with a single synaptic population, and no intercompartment competition existed. Note that when CC approached 1, the total area of the modeled system approximately doubled, and therefore the total conductance of each type of channels was effectively halved. This greatly diminished the capability of this model to generate both types of spikes at CC values close to 1, rendering the measurement of the average synaptic weights at these values problematic.

Once coupling between compartments is strong enough for competition to exist, channel density at the respective compartments determines which compartment would impact the other compartment more strongly and thus determines the identity of the dominating group of synapses. In Fig. 5*C*, the CC was set to 0.7, and the dendritic $\bar{g}_{Na}$ was 50 pS/μm^2. When $\bar{g}_{LVA\text{-}Ca}$ was lower than 27 pS/μm^2, the somatic synapses became dominant, whereas with higher $\bar{g}_{LVA\text{-}Ca}$ values dendritic synapses dominated. For instance, at $\bar{g}_{LVA\text{-}Ca}$ = 20 pS/μm^2 (Fig. 5*C*, black vertical line), the average synaptic weight was 0.54 at the soma (Fig. 5*C*, blue) and 0.12 at the dendrite (Fig. 5*C*, red). With increasing $\bar{g}_{LVA\text{-}Ca}$, progressively more dendritic synapses were strengthened, whereas somatic synapses were gradually depressed. At $\bar{g}_{LVA\text{-}Ca}$ = 40 pS/μm^2 (Fig. 5*C*, gray vertical line), the average w was 0.056 at the soma and 0.82 at the dendrite. The difference between low and high $\bar{g}_{LVA\text{-}Ca}$ values was rooted in the source of Ca^{2+} spike generation. With $\bar{g}_{LVA\text{-}Ca} <$ 27 pS/μm^2, the BPAP was necessary for the initiation of a Ca^{2+} spike, a condition leading to somatic dominance. With higher $\bar{g}_{LVA\text{-}Ca}$ values, dendritic input alone was enough to trigger a Ca^{2+} spike, resulting in dendritic dominance.

To quantify the effect of the somatic spike on the dendritic spike and vice versa, we calculated the normalized cross-correlation between the two types of spikes (Fig. 5*D*). With $\bar{g}_{LVA\text{-}Ca}$ = 20 pS/μm^2 (Fig. 5*D*, black), the Na^+ spike tended to occur before the Ca^{2+} spike, whereas at $\bar{g}_{LVA\text{-}Ca}$ = 40 pS/μm^2, no Na^+ spike preceded the dendritic Ca^{2+} spike (Fig. 5*D*, gray). This implies that only with low $\bar{g}_{LVA\text{-}Ca}$ is the BPAP required for Ca^{2+} spike induction. The multiple peaks with large $\bar{g}_{LVA\text{-}Ca}$ values (Fig. 5*D*, gray) indicate that each Ca^{2+} spike caused more somatic action potentials than it did at low values (Fig. 5*D*, black). As more somatic spikes were induced by an external source (namely the Ca^{2+} spike) rather than by local somatic inputs, more somatic synapses were depressed due to being uncorrelated with their STDP-inducing signal.

We concluded that two conditions must be fulfilled for competition to ensue between two synaptic populations, each with its respective STDP-inducing signal: *1*) the effective coupling between the two regions must be sufficiently strong so that the spike in at least one compartment significantly affects spiking probability in the other compartment; and *2*) synapses in at least one compartment must be potent enough to produce local spikes. Only under these two conditions can one synaptic population dominate the other population by decorrelating the other synapses from their own plasticity-inducing signal.

Competition in a symmetrical simplified model. To eliminate all asymmetries inherent to different spike mechanisms at the soma and dendrite, we examined whether competition may also occur in a symmetrical case consisting of two electrically coupled identical compartments, both with identical Na^+ spike mechanisms and an identical number of synapses (Fig. 6*A*; see MATERIALS AND METHODS). In this model, a bifurcation point exists: above a critical value of electrical coupling strength (CC = 0.4), competition emerged between the synapses of different compartments, which led to the complete dominance of one group of synapses over the other. Because of the complete symmetry between compartments, the dominating group of synapses alternated randomly between both synaptic populations (Fig. 6*B*). We calculated spike coupling between compartments at steady state (see MATERIALS AND METHODS) and found that for $CC > 0.4$, spike firing in one compartment became completely dominated by the spike firing in the other compartment (Fig. 6*C*, red or blue). Synapses in the compartment that dominated firing eventually won the competition (Fig. 6*B*). At the bifurcation point (CC = 0.4), there was already a steep increase in spike coupling without synaptic activity (Fig. 6*C*, black line; see MATERIALS AND METHODS). This indicated that sufficiently strong spike coupling between compartments was enough to trigger competition between synaptic populations, even in the symmetrical case with two identical STDP-inducing signals.

We ran simulations using a weight-dependent (multiplicative) STDP rule (van Rossum et al. 2000; Gutig et al. 2003; see MATERIALS AND METHODS) and found similar interregional competition as for the additive rule (see MATERIALS AND METHODS). We also simulated cases with different plasticity rules in each compartment: *1*) the time constant for plasticity (τ) was varied from 10 to 50 ms for one of the compartments while keeping τ = 20 ms in the other compartment; and *2*) the amplitude of synaptic potentiation and depression (A_+ and A_-) was increased by a factor of 1.5–3 in one of the compartments. In all cases, competition between the two synaptic populations persisted and ensued at the same value of CC (0.4) as found when using the same STDP rule in both compartments (results not shown).

DISCUSSION

Inspired by recent experimental results demonstrating the existence of multiple regional signals for synaptic plasticity in single neurons, we explored this case in both detailed and simplified neuron models. We focused on models consisting of two regional spikes, each inducing STDP. It was assumed, for the sake of simplicity, that both synaptic populations obeyed the same plasticity rule. The general finding was that as soon as the two regional signals started interacting (strong spike coupling between regions), competition ensued between the two respective synaptic populations, and one group of synapses

Downloaded from jn.physiology.org on March 22, 2011

tended to eventually dominate by becoming strong at the expense of weakening the other group of synapses.

Competition between synaptic populations in different regions of the same cell fundamentally differs from competition between synapses within one population of synapses with a single plasticity-inducing signal. Within a single population, all synapses have the same probability to be potentiated (or depressed). In contrast, with two synaptic populations in two electrically coupled regions of the same neuron, the probability of the synapses to be potentiated or depressed is different for each population of synapses. As we show in the symmetrical two-compartment model (Fig. 6), at steady state, synapses in one group have a greater chance of strengthening than synapses in the other group, even though they are completely identical and all synapses experience the same learning rule.

This interregional competition was robust, appearing in both detailed and simplified models of L5 pyramidal cells, consisting of Na^+ and Ca^{2+} spikes as STDP-inducing signals. Regional competition was also apparent for symmetrical systems containing two identical compartments, both having a regional Na^+ spike serving as the STDP signal, as well as in a two-compartment model with an integrate-and-fire spike mechanism (results not shown). In these latter cases, a random advantage for synapses in one compartment resulted in symmetry breaking, leading to competition and, with a sufficiently strong effective coupling, the domination of one group of synapses over the other. Hence, the inherent differences in the properties of different types of the STDP-inducing signals (such as spike threshold, total charge, etc.) do not play a key role in the emergence of competition between the two synaptic populations.

Other synaptic plasticity signals have been suggested to operate in the dendrites, such as local voltage (Lisman and Spruston 2005; Hardie and Spruston 2009) and intracellular calcium concentration (Shouval et al. 2002; Froemke et al. 2005). We also simulated the case, whereby either the local membrane potential or the local Ca^{2+} concentration served as the plasticity-inducing signal. We used either the local voltage or calcium concentration to detect the onset of a Ca^{2+} spike; when either the voltage or calcium concentration surpassed a predetermined threshold, synaptic plasticity ensued. We found that interregional competition exists in both cases (results not shown). Hence, the existence of this type of competition does not depend on the particular STDP-inducing signal used in this work. Moreover, we ran simulations with a temporally reversed STDP rule in the "dendritic" compartment for the case of two-compartment model (as in Fig. 5). In this scenario, inputs preceding the Ca^{2+} spike underwent synaptic depression, whereas inputs following the spike were potentiation. The magnitude of potentiation was set to be larger than depression (by switching between values of A_+ and A_-; see *Eq. 2*). Results were consistent with simulations using the regular STDP rule, whereby intercompartment competition emerged at a critical value of coupling (CC = 0.6, results not shown).

All attributes of interregional competition were also reproduced when we used a multiplicative (weight-dependent) rather than an additive STDP rule in all three models used in this study. The same holds true when using different STDP rules in each compartment such as a different time constant for plasticity (τ) and a different amplitude of synaptic potentiation/depression ($A_{+/-}$). Thus our findings highlight a general principle, independent of the particular STDP rule used, specifically that interregional competition among synapses is inherent to the case, whereby multiple plasticity-inducing signals operate at different dendritic regions.

We propose that the emergence of competition between two synaptic populations can be experimentally tested in pair recordings from the somata of two L5 pyramidal cells. These cells would be effectively coupled by artificially injecting a BPAP-like pulse in cell 2 following a somatic Na^+ spike in cell 1 and vice versa. The amplitude of the triggered pulse could be adjusted to represent the strength of coupling between the cells, thus practically simulating the symmetrical case depicted in Fig. 6. We predict that for a threshold value of such coupling between cells, competition would ensue between their synaptic populations, leading to potentiation of the synapses of one cell at the expense of diminishing the strength of synapses in the other cell. By focusing on two cells rather than on two regions within the same cell, one would be able to demonstrate that interregional competition is inherent to a system with two interacting plasticity supervisors and does not require complex effects of cell morphology or of interaction between different spike types.

Furthermore, as we suggest that a key role for the BPAP in L5 pyramidal cells is to maintain the balance between proximal and distal synapses, we predict that in an experiment using cortical slices under conditions of high activity similar to the in vivo state (Destexhe et al. 2001), enhancing the invasion of the BPAP into the apical tuft [e.g., by partial blockade or inactivation of apical potassium channels (Hoffman et al. 1997)] would affect the interdendritic competition, resulting in a new steady-state distribution of synaptic efficacies. In particular, rather than having a homogenous weight distribution of synapses as found by Williams and Stuart (2002), we expect distal synapses to become weaker that proximal synapses. In contrast, substantially decreasing the amplitude of the BPAP (e.g., by puffing local TTX in the apical stem dendrite) would lead to an increase in synaptic efficacies in apical regions at the expense of somatic synapses.

Synaptic democracy with competing regional plasticity signals. Interregional competition resulted in most cases in a lack of balance of synaptic efficacies throughout the neuron. In L5 pyramidal cell models, the broader dendritic Ca^{2+} spikes generate more somatic Na^+ spikes than vice versa. This implies that distal synapses will tend to dominate proximal synapses in contrast to the experimental finding that in L5 pyramidal cells, the strength (conductance) of both proximal and distal synapses seems to be uniformly distributed throughout the dendritic tree (Williams and Stuart 2002). We have demonstrated that by controlling the degree of coupling between the two competing regions, such a balance of synaptic efficacies can be achieved. We show that the cell synapses would "survive" the interregional competition if the coincidence of BPAPs and the activation of apical synapses is required for the initiation of dendritic Ca^{2+} spikes, as was found to be the case in vitro (Larkum et al. 1999a; Larkum et al. 1999b, 2001).

However, strong local depolarizing current to the apical tree was shown to independently produce Ca^{2+} spikes without the requirement of BPAPs, suggesting that correlated excitatory inputs could generate Ca^{2+} spikes (Schiller et al. 1997; Stuart et al. 1997a; Helmchen et al. 1999; Larkum and Zhu 2002). On

Downloaded from jn.physiology.org on March 22, 2011

the other hand, activation of high-frequency somatic Na^+ spikes has been shown to generate calcium electrogenesis in the apical dendrite without the need for distal inputs (Stuart et al. 1997a; Larkum et al. 1999b; Williams and Stuart 1999). In these two cases, interregional competition would lead to either distal or proximal dominance, respectively. However, it remains to be examined whether such independent Ca^{2+} spikes are also generated in vivo. Moreover, even if in vivo distal dendritic Ca^{2+} spikes are initiated independently, they may remain restricted to the distal dendrite and not affect somatic firing, for example, via the active uncoupling of distal and proximal regions by inhibitory inputs (Miles et al. 1996; Tsubokawa and Ross 1996). In this case, competition between regions would not take place. Such electrically isolated Ca^{2+} spikes have indeed been shown in vitro (Schiller et al. 1997; Wei et al. 2001; Larkum and Zhu 2002).

Other mechanisms may operate in dendrites for maintaining synaptic democracy even in the presence of interregional competition. One such mechanism is homeostatic synaptic plasticity (HSP; Lissin et al. 1998; O'Brien et al. 1998; Turrigiano et al. 1998). However, the time constant for HSP is typically too long (hours to days), compared with the STDP mechanism, to counteract the effect of STDP (Turrigiano et al. 1998; Rabinowitch and Segev 2006). Another possible mechanism for achieving synaptic democracy is the anti-Hebbian STDP mechanism as suggested by Rumsey and Abbott (2004, 2006). Synaptic democracy could also be maintained throughout the dendritic tree by scaling the upper limit of synaptic conductance with distance from the soma (Gidon and Segev 2009) or by having different forms of metaplasticity (Abraham and Bear 1996) at different cell regions.

Regional competition with different synaptic plasticity rules. The distal dendritic Ca^{2+} spikes, rather than the BPAPs, were used in this study as STDP-inducing signals for distal synapses. Dendritic Ca^{2+} spikes have been shown to trigger both LTP and LTD in pyramidal cells (Golding et al. 2002), whereas the BPAPs tend to fail in invading the distal dendritic region (Markram et al. 1997; Larkum et al. 2001), and inhibition can block the BPAP completely (Larkum et al. 1999a). It is therefore unlikely that the BPAP provides a global and robust plasticity signal to all synapses and only natural that distal synapses have their own regional plasticity-inducing signal (Golding et al. 2002; Kampa et al. 2006; Letzkus et al. 2006; Sjöström and Häusser 2006; Remy and Spruston 2007; Takahashi and Magee 2009).

However, we still lack the experimental characterization of the learning rules governing Ca^{2+} spike-induced synaptic plasticity. Here, we assumed that Ca^{2+} spikes induce STDP as do somatic Na^+ spikes. It is important to note that the assumption that Ca^{2+} spike triggers plasticity is not a prerequisite for interregional competition. The mere fact that somatic spikes can be induced by either proximal inputs or dendritic spikes is sufficient to induce synaptic competition between cell regions. Thus, even if STDP was triggered only by Na^+ spikes for proximal synapses and the Ca^{2+} spikes did not induce plasticity, proximal synapses were still depressed (in the conditions under which Ca^{2+} spikes generate somatic bursts), and thus distal synapses still dominated proximal synapses (results not shown). Indeed, different plasticity-inducing signals such as NMDA spikes (Schiller et al. 2000; Schiller and Schiller 2001; Ariav et al. 2003; Larkum et al. 2009) and sodium spikes (Turner et al. 1991; Stuart et al. 1997a; Golding and Spruston 1998; Gasparini et al. 2004) exist in dendrites, and therefore different plasticity rules are likely to exist at different cell regions. As they become better characterized experimentally, it would be interesting to explore their implications for the coexistence of synaptic democracy throughout the dendritic tree using computational studies.

ACKNOWLEDGMENTS

We warmly thank Yosef Yarom, Israel Nelken, Jackie Schiller, Arnd Roth, Haim Sompolinsky, and Robert Gutig for useful discussions in different stages of this work.

GRANTS

This work was supported by a grant from the Israel Science Foundation and by the Blue Brain Project.

DISCLOSURES

No conflicts of interest, financial or otherwise, are declared by the author(s).

REFERENCES

Abbott LF, Nelson SB. Synaptic plasticity: taming the beast. *Nat Neurosci* 3, *Suppl*: 1178–1183, 2000.

Abraham WC, Bear MF. Metaplasticity: the plasticity of synaptic plasticity. *Trends Neurosci* 19: 126–130, 1996.

Ariav G, Polsky A, Schiller J. Submillisecond precision of the input-output transformation function mediated by fast sodium dendritic spikes in basal dendrites of CA1 pyramidal neurons. *J Neurosci* 23: 7750–7758, 2003.

Bell CC, Han VZ, Sugawara Y, Grant K. Synaptic plasticity in a cerebellum-like structure depends on temporal order. *Nature* 387: 278–281, 1997.

Bi GQ. Spatiotemporal specificity of synaptic plasticity: cellular rules and mechanisms. *Biol Cybern* 87: 319–332, 2002.

Buzsáki G, Penttonen M, Nádasdy Z, Bragin A. Pattern and inhibition-dependent invasion of pyramidal cell dendrites by fast spikes in the hippocampus in vivo. *Proc Natl Acad Sci USA* 93: 9921–9925, 1996.

Dan Y, Poo MM. Spike timing-dependent plasticity: from synapse to perception. *Physiol Rev* 86: 1033–1048, 2006.

Debanne D, Gähwiler BH, Thompson SM. Long-term synaptic plasticity between pairs of individual CA3 pyramidal cells in rat hippocampal slice cultures. *J Physiol* 507: 237–247, 1998.

Destexhe A, Rudolph M, Fellous JM, Sejnowski TJ. Fluctuating synaptic conductances recreate in vivo-like activity in neocortical neurons. *Neuroscience* 107: 13–24, 2001.

Feldman DE. Timing-based LTP and LTD at vertical inputs to layer II/III pyramidal cells in rat barrel cortex. *Neuron* 27: 45–56, 2000.

Froemke RC, Poo MM, Dan Y. Spike-timing-dependent synaptic plasticity depends on dendritic location. *Nature* 434: 221–225, 2005.

Gasparini S, Migliore M, Magee JC. On the initiation and propagation of dendritic spikes in CA1 pyramidal neurons. *J Neurosci* 24: 11046–11056, 2004.

Gerstner W, Kempter R, van Hemmen JL, Wagner H. A neuronal learning rule for sub-millisecond temporal coding. *Nature* 383: 76–81, 1996.

Gidon A, Segev I. Spike-timing-dependent synaptic plasticity and synaptic democracy in dendrites. *J Neurophysiol* 101: 3226–3234, 2009.

Goldberg J, Holthoff K, Yuste R. A problem with Hebb and local spikes. *Trends Neurosci* 25: 433–435, 2002.

Golding NL, Spruston N. Dendritic sodium spikes are variable triggers of axonal action potentials in hippocampal CA1 pyramidal neurons. *Neuron* 21: 1189–1200, 1998.

Golding NL, Staff NP, Spruston N. Dendritic spikes as a mechanism for cooperative long-term potentiation. *Nature* 418: 326–331, 2002.

Gutig R, Aharonov R, Rotter S, Sompolinsky H. Learning input correlations through nonlinear temporally asymmetric Hebbian plasticity. *J Neurosci* 23: 3697–3714, 2003.

Hardie J, Spruston N. Synaptic depolarization is more effective than back-propagating action potentials during induction of associative long-term potentiation in hippocampal pyramidal neurons. *J Neurosci* 29: 3233–3241, 2009.

Downloaded from jn.physiology.org on March 22, 2011

Helmchen F, Svoboda K, Denk W, Tank DW. In vivo dendritic calcium dynamics in deep-layer cortical pyramidal neurons. *Nat Neurosci* 2: 989–996, 1999.

Hines ML, Carnevale NT. The NEURON simulation environment. *Neural Comput* 9: 1179–1209, 1997.

Hodgkin AL, Huxley AF. Propagation of electrical signals along giant nerve fibers. *Proc R Soc Lond B Biol Sci* 140: 177–183, 1952.

Hoffman DA, Magee JC, Colbert CM, Johnston D. K^+ channel regulation of signal propagation in dendrites of hippocampal pyramidal neurons. *Nature* 387: 869–875, 1997.

Holthoff K, Kovalchuk Y, Konnerth A. Dendritic spikes and activity-dependent synaptic plasticity. *Cell Tissue Res* 326: 369–377, 2006.

Holthoff K, Kovalchuk Y, Yuste R, Konnerth A. Single-shock LTD by local dendritic spikes in pyramidal neurons of mouse visual cortex. *J Physiol* 560: 27–36, 2004.

Kampa BM, Letzkus JJ, Stuart GJ. Requirement of dendritic calcium spikes for induction of spike-timing-dependent synaptic plasticity. *J Physiol* 574: 283–290, 2006.

Kim HG, Connors BW. Apical dendrites of the neocortex: correlation between sodium- and calcium-dependent spiking and pyramidal cell morphology. *J Neurosci* 13: 5301–5311, 1993.

Larkum ME, Zhu JJ. Signaling of layer 1 and whisker-evoked Ca^{2+} and Na^+ action potentials in distal and terminal dendrites of rat neocortical pyramidal neurons in vitro and in vivo. *J Neurosci* 22: 6991–7005, 2002.

Larkum ME, Rioult MG, Luscher HR. Propagation of action potentials in the dendrites of neurons from rat spinal cord slice cultures. *J Neurophysiol* 75: 154–170, 1996.

Larkum ME, Kaiser KM, Sakmann B. Calcium electrogenesis in distal apical dendrites of layer 5 pyramidal cells at a critical frequency of back-propagating action potentials. *Proc Natl Acad Sci USA* 96: 14600–14604, 1999a.

Larkum ME, Zhu JJ, Sakmann B. A new cellular mechanism for coupling inputs arriving at different cortical layers. *Nature* 398: 338–341, 1999b.

Larkum ME, Zhu JJ, Sakmann B. Dendritic mechanisms underlying the coupling of the dendritic with the axonal action potential initiation zone of adult rat layer 5 pyramidal neurons. *J Physiol* 533: 447–466, 2001.

Larkum ME, Nevian T, Sandler M, Polsky A, Schiller J. Synaptic integration in tuft dendrites of layer 5 pyramidal neurons: a new unifying principle. *Science* 325: 756–760, 2009.

Letzkus JJ, Kampa BM, Stuart GJ. Learning rules for spike timing-dependent plasticity depend on dendritic synapse location. *J Neurosci* 26: 10420–10429, 2006.

Lisman J, Spruston N. Postsynaptic depolarization requirements for LTP and LTD: a critique of spike timing-dependent plasticity. *Nat Neurosci* 8: 839–841, 2005.

Lissin DV, Gomperts SN, Carroll RC, Christine CW, Kalman D, Kitamura M, Hardy S, Nicoll RA, Malenka RC, von Zastrow M. Activity differentially regulates the surface expression of synaptic AMPA and NMDA glutamate receptors. *Proc Natl Acad Sci USA* 95: 7097–7102, 1998.

Markram H, Lübke J, Frotscher M, Sakmann B. Regulation of synaptic efficacy by coincidence of postsynaptic APs and EPSPs. *Science* 275: 213–215, 1997.

Miles R, Toth K, Gulyas AI, Hajos N, Freund TF. Differences between somatic and dendritic inhibition in the hippocampus. *Neuron* 16: 815–823, 1996.

O'Brien RJ, Kamboj S, Ehlers MD, Rosen KR, Fischbach GD, Huganir RL. Activity-dependent modulation of synaptic AMPA receptor accumulation. *Neuron* 21: 1067–1078, 1998.

Rabinowitch I, Segev I. The interplay between homeostatic synaptic plasticity and functional dendritic compartments. *J Neurophysiol* 96: 276–283, 2006.

Remy S, Spruston N. Dendritic spikes induce single-burst long-term potentiation. *Proc Natl Acad Sci USA* 104: 17192–17197, 2007.

Rumsey CC, Abbott LF. Equalization of synaptic efficacy by activity- and timing-dependent synaptic plasticity. *J Neurophysiol* 91: 2273–2280, 2004.

Rumsey CC, Abbott LF. Synaptic democracy in active dendrites. *J Neurophysiol* 96: 2307–2318, 2006.

Schaefer AT, Larkum ME, Sakmann B, Roth A. Coincidence detection in pyramidal neurons is tuned by their dendritic branching pattern. *J Neurophysiol* 89: 3143–3154, 2003.

Schiller J, Schiller Y. NMDA receptor-mediated dendritic spikes and coincident signal amplification. *Curr Opin Neurobiol* 11: 343–348, 2001.

Schiller J, Helmchen F, Sakmann B. Spatial profile of dendritic calcium transients evoked by action potentials in rat neocortical pyramidal neurones. *J Physiol* 487: 583–600, 1995.

Schiller J, Schiller Y, Stuart G, Sakmann B. Calcium action potentials restricted to distal apical dendrites of rat neocortical pyramidal neurons. *J Physiol* 505: 605–616, 1997.

Schiller J, Major G, Koester HJ, Schiller Y. NMDA spikes in basal dendrites of cortical pyramidal neurons. *Nature* 404: 285–289, 2000.

Schwindt P, Crill W. Mechanisms underlying burst and regular spiking evoked by dendritic depolarization in layer 5 cortical pyramidal neurons. *J Neurophysiol* 81: 1341–1354, 1999.

Shouval HZ, Bear MF, Cooper LN. A unified model of NMDA receptor-dependent bidirectional synaptic plasticity. *Proc Natl Acad Sci USA* 99: 10831–10836, 2002.

Sjöström PJ, Häusser M. A cooperative switch determines the sign of synaptic plasticity in distal dendrites of neocortical pyramidal neurons. *Neuron* 51: 227–238, 2006.

Song S, Miller KD, Abbott LF. Competitive Hebbian learning through spike-timing-dependent synaptic plasticity. *Nat Neurosci* 3: 919–926, 2000.

Spruston N, Schiller Y, Stuart G, Sakmann B. Activity-dependent action potential invasion and calcium influx into hippocampal CA1 dendrites. *Science* 268: 297–300, 1995.

Stuart G, Schiller J, Sakmann B. Action potential initiation and propagation in rat neocortical pyramidal neurons. *J Physiol* 505: 617–632, 1997a.

Stuart G, Spruston N, Sakmann B, Häusser M. Action potential initiation and backpropagation in neurons of the mammalian CNS. *Trends Neurosci* 20: 125–131, 1997b.

Stuart GJ, Sakmann B. Active propagation of somatic action potentials into neocortical pyramidal cell dendrites. *Nature* 367: 69–72, 1994.

Takahashi H, Magee JC. Pathway interactions and synaptic plasticity in the dendritic tuft regions of CA1 pyramidal neurons. *Neuron* 62: 102–111, 2009.

Tsubokawa H, Ross WN. IPSPs modulate spike backpropagation and associated $[Ca^{2+}]_i$ changes in the dendrites of hippocampal CA1 pyramidal neurons. *J Neurophysiol* 76: 2896–2906, 1996.

Turner RW, Meyers DE, Richardson TL, Barker JL. The site for initiation of action potential discharge over the somatodendritic axis of rat hippocampal CA1 pyramidal neurons. *J Neurosci* 11: 2270–2280, 1991.

Turrigiano GG, Leslie KR, Desai NS, Rutherford LC, Nelson SB. Activity-dependent scaling of quantal amplitude in neocortical neurons. *Nature* 391: 892–896, 1998.

van Rossum MC, Bi GQ, Turrigiano GG. Stable Hebbian learning from spike timing-dependent plasticity. *J Neurosci* 20: 8812–8821, 2000.

Wei DS, Mei YA, Bagal A, Kao JP, Thompson SM, Tang CM. Compartmentalized and binary behavior of terminal dendrites in hippocampal pyramidal neurons. *Science* 293: 2272–2275, 2001.

Williams SR, Stuart GJ. Mechanisms and consequences of action potential burst firing in rat neocortical pyramidal neurons. *J Physiol* 521: 467–482, 1999.

Williams SR, Stuart GJ. Dependence of EPSP efficacy on synapse location in neocortical pyramidal neurons. *Science* 295: 1907–1910, 2002.

Zhang LI, Tao HW, Holt CE, Harris WA, Poo M. A critical window for cooperation and competition among developing retinotectal synapses. *Nature* 395: 37–44, 1998.

Downloaded from jn.physiology.org on March 22, 2011